Effects of Ionizable Groups on the Redox Potentials of Cytochrome c_3 from *D. vulgaris* Miyazaki F

Jang-Su Park* and Shin Won Kang

Department of Chemistry, Pusan National University, Pusan 609-735, Korea
Received May 3, 1996

The p^2H dependence of the NMR chemical shifts of the proton signals of heme methyl groups and ionizable groups in the vicinity of the heme were investigated. The p^2H titration of heme methyl signals in four macroscopic oxidation states by saturation tranfer method was performed in the range between p^2H 5.2 and 9.0. While the p^2H dependence of the heme methyl resonance in fully oxidized state was small, most resonances in the intermediate oxidation states showed certain shifts. Particularly, methyl resonances of heme 1 (sequential heme numbering) exhibited sharp p^2H dependence in acidic range. β-CH_2 of the propionate of hemes 1 and 4 were titrated in the range of p^2H 4.5-9.0. Only the 6-propionate group of heme 1 was protonated in this p^2H range and its titration curve was similar to those of methyl resonances of heme 1 in intermediate oxidation states. Analysis of the microscopic redox potentials showed that they change depending on p^2H. The ionizable groups responsible for the p^2H dependence of these potentials are 6-propionate of heme 1 in acidic range and His 67 in basic range.

Introduction

Cytochromes c_3, isolated from a sulfate-reducing bacterium, possesses four c-type hemes per molecule. Cytochrome c_3 is involved in the electron-transport system in the bacteria as a partner of hydrogenase. Some remarkable properties of cytochrome c_3 from *D. vulgaris* Miyazaki F(*Dv*MF) have been reported. This protein shows low redox protentials in comparison with other c-type cytochromes.[1] The heterogenous electon-transfer rates at various electrodes are very rapid.[2,3] The electric conductance of a dry film of ferrocytochrome c_3 is as high as 0.02 S cm^{-1} in the fully reduced state.[4] The ionization potential of solid state ferricytochrome c_3 is 0.7 eV lower than that of ferricytochrome c.[5]

Although extensive investigations of this protein have been carried out using a wide variety of physicochemical methods, the significance of the four hemes remains obscure. The key in understanding of the properties mentioned above is to elucidate the roles of each of the four hemes.

Since cytochrome c_3 has four redox centers, four macroscopic redox potentials and thirty two microscopic redox potentials can be defined.[6] The macroscopic redox potentials of cytochrome c_3 (*Dv*MF) were determined by electrochemical methods (potentiometry or differential pulse polargraphy)[1] and NMR.[7] The chemical shifts of eight heme methyl signals in NMR spectra were determined for five macroscopic oxidation states by saturation transfer method. This results were used for the calculation of the electron distribution probability at each heme in the five macroscopic oxidation states. The combined use of the macroscopic redox potentials with the electron distribution probabilities enabled estimation of the 32 microscopic redox potentials.[6] The assignment of redox potentials to each heme in the crystal has been established.[8]

Since the crystal structure of this protein is available at 1.8 Å resolution,[9] the relationship between its structure and

redox behavior can be discussed in detail. The aim of this work is to make clear the structural factors which determine the redox potentials of each of the four hemes. In this paper, the pH dependence of the NMR chemical shifts of the proton signals of heme methyl groups and ionizable groups in the vicinity of the hemes will be discussed in the light of tertiary structural information.

Materials and Methods

Desulfovibrio vulgaris Miyazaki F was cultured in medium C.[10] Cytochrome c_3 was purified according to the procedure reported previously.[11] The purity index (A_{552}(red)/A_{280}(ox)) of the final sample was over 3.0. The purity was confirmed also by SDS-poylacrylamide gel electrophoresis. In NMR experiments, a trace amount of hydrogenase was added to a 1.3 mM cytochrome c_3 solution (molar ratio of *ca*. 0.001) as a redox catalyst. The hydrogenase was extracted from *D. vulgaris* Miyazaki F, and purified as reported elsewhere.[12] Partial reduction (referred to as an intermediate redox stage hereafter) of a cytochrome c_3 solution was achieved by controlling the partial pressure of hydrogen and argon gases in an NMR tube. In preparation of the sample for NMR measurements, 30 mM phosphate and 30 mM borate-NaO^{2}H were used for p^2H 5.2-8.8 and p^2H 9.0-9.2, respectively. Otherwise, pH was adjusted by addition of a concentrated NaO^{2}H or ^{2}HCl solution. The p^2H valuse cited in this paper are direct reading on a pH meter.

^{1}H NMR spectra were obtained on a Brucker AM 400 MHz spectrometer at 30 °C. Chemical shifts are presented in parts per million relative to the internal standard of 2,2-dimethyl-2-sillapentane-5-sulfonate (DSS). Saturation transfer experiments were carried out for various intermediate redox stages in order to assign heme methyl resonances in the five macroscopic oxidation states. Sixteen free induction decays (FID) were accumulated repeatedly under on-resonance and off-resonance irradiation for 1s. The irradiation was adjusted to suppress the signal intensity to half the original

---

one. One thousand transients were accumulated for each FID.

Differential pulse polarograms (DPP) were measured at a dropping mercury electrode with a potentiostat, Fuso polarograph Model 312. Modulation amplitude, sweep rate, drop time, and sampling time were 10 mV, 2 mVs⁻¹, 2s, and 20 ms, respectively.

Potentials referring to the normal hydrogen electrode at 30 ℃ were presented in this work.

Results

p²H dependence of the heme methyl chemical shifts. The general features of the NMR spectra of cytochrome c_3 from *D. vulgaris* Miyazaki F, in the various redox stages were discussed previously.[6,7] The assignment of the heme methyl signals has been established.[13] Namely,

heme 1(h2′); B, F, G and M,
heme 2(h3′); C and D,
heme 3(h4′); E and J,
heme 4(h1′); A, H, I and K,

where hemes were numbered according to the sequential heme numbering. The heme numbering in the parenthesis is due to the order of the major reduction.[13] The p²H titration of these signals in four macroscopic oxidation states were performed in the range between p²H 5.2 and 9.2. The chemical shifts in the intermediate oxidation states were determined by saturation transfer method. The obtained chemical shifts of heme methyl resonances were plotted as a function of p²H in Figure 1.

While the p²H dependence of the heme methyl resonances in the fully oxidized state (S_0) is small, most resonances in the intermediate oxidation states showed certain shifts, especially in one and two-electron reduction states (S_1 and S_2). Particularly, methyl resonances of heme 1 exhibited significant p²H dependence in acidic range. The pK_a values were determined by nonlinear least-squares fitting calculation for several signals. The obtained pK_a values of signals B, F and G in one-electron reduction states were 5.5, 6.1 and 5.9, respectively and those in two electron reduction states were 6.3, 6.5 and 6.5, respectively. This results showed that the values of pK_a are not constant upon the change of the oxidation states of the protein.

The p²H dependence of the chemical shifts of the heme methyl signals in intermediate oxidation states implies that the midpoint redox potential of each of the hemes changes with p²H.

p²H titration of propionate β-CH₂. The assignments of the signals of heme propionic acid groups in cytochrome c_3 were carried out on the basis of 1D NOE and 2D DQF-COSY, HOHAHA spectra spectra.[11] Since methyl signals of heme 1 and heme 4 showed significant pH dependence in acidic range as shown in Figure 1. β-CH₂ of the propionate of hemes 1 and 4 were titrated in the range of p²H 4.5-9.0. The chemical shifts of β-CH₂ could be followed by measuring 2D-HOHAHA spectra. Their chemical shifts were plotted as a function of p²H in Figure 2.

Only 6-propionate group of heme 1 was protonated in the p²H range of 5.0-9.0. The pK_a values determined by nonlinear least-squares fitting were 5.9 and 6.0 for β₁-H and β₂-H, res-
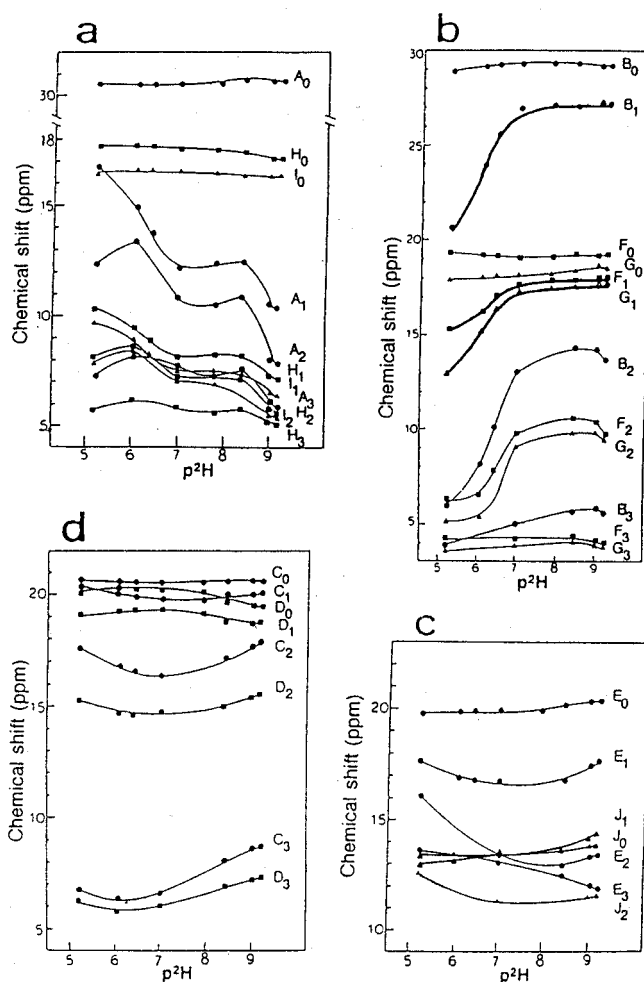

Figure 1. p²H dependence of the chemical shifts of four hemes methyl group resonances, in different oxidation states at 30 ℃. a, heme 4 (h1′); b, heme 1 (h2′); c, heme 2 (h3′); d, heme 3 (h4′). The heme numbering in the parenthesis is due to the order of the major redution. The subscripts of the labls of heme methyl signals denotes the macroscopic oxidation states. For example, A_i is heme methyl signal A in the *i*-electron redution state (A_0 is for the fully-oxidized state).

pectively.

The pK_a values of 6-propionate group of heme 1 are in good agreement with those of the methyl groups of heme 1 in the one-electron reduction state.

p²H dependence of macroscopic redox potentials.

A tetraheme protein, such as cytochrome c_3, has five macroscopic oxidation states: S_0, S_1, S_2, S_3 and S_4 states and four macroscopic redox potentials, E^0_i (i=1-4), can be defined as

$$E = E^0_i + (RT/F)\ln(f_{i-1}/f_i) \qquad (1)$$

where E, R, F, T and f_i are the equilibrium potential, gas constant, Faraday constant, absolute temperature and mole fraction of cytochrome c_3 in the *i*-electron reduced state, respectively.

The macroscopic redox potentials of the cytochrome c_3 molecule from *D. vulgaris* Miyazaki F were evaluated using
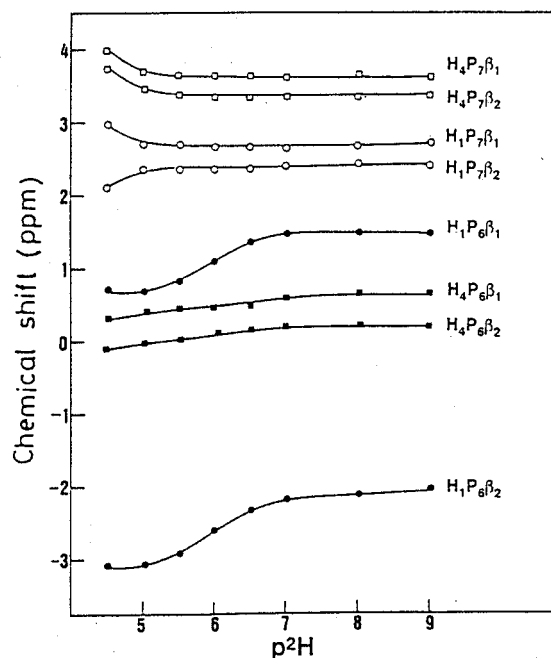
Figure 2. p^2H dependence of the chemical shifts of β-CH_2 of the propionate of heme 4 (h1′) and 1 (h2′). The closed and open squares represent the 6- and 7-propionate of heme 4, respectively. The closed and open circles represent the 6- and 7-propionate of heme 1, respectively.

Figure 3. The four macroscopic redox potentials of cytochrome c_3 from D.v.MF, determined by differential pulse polarography at 30 ℃. E_i^o and NHE denote the macroscopic formal redox potential at the i-th redution step and the normal hydorgen electrode, respectively.

least-squares fitting of the differential pulse polarogram to the analytical equation for the four consecutive one-electron reversible electrode reaction. The calculation procedure was reported in previous publication.[14] The results at p^2H 9.0 (30 mM phosphate buffer). p^2H 7.1 (30 mM phosphate buffer) and p^2H 9.0 (30 mM borate-NaO^2H buffer) are shown in Figure 3.

$E^0{}_i'$ represents the macroscopic redox potential for the ith one-electron redox process. Note that the potential differences between $E_2^{0''}$ and $E_0^{3'}$ are greater at p^2H 5.2 and p^2H 9.0 than that at p^2H 7.1. Expect for $E^0{}_i'$ the values of $E^0{}_i'$ shifts toward negative direction with the increase of pH.

p^2H dependence of microscopic redox potentials and interacting potentials. As indicated elsewhere,[6] five sets of spectra of cytochrome c_3 corresponding to the five macroscopic oxidation states appeared and disappeared one after another. In the intermediate oxidation states, the signals of the heme methyl groups appeard in the region between the positions for the fully oxidized and fully reduced states. Furthermore, only one signal was observed in a saturation transfer experiment for a specific methyl group in each oxidation state. These facts indicate that the transferred electron is delocalized among the four hemes and is hopping around at a rate faster than the NMR time scale.[7,13,15] Thus, the spectra include the information on the electron distribution probability at each heme, which can be used for determination of the microscopic redox potenrials.

If one denotes each heme as o (for oxidized) or r (for reduced), the microscopic redox potentials for the first reduction step, e_i^I (i=1-4; heme numbering), can be defined as follows
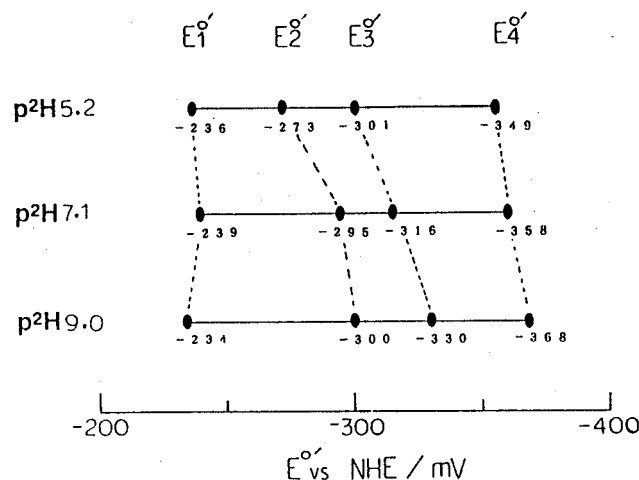
where [oroo], for example, stands for the concentration of the redox species, in which only heme 2 is reduced. From these equations it is easy to obtain

$$E = e_1^I + (RT/F)\ln([oooo]/[rooo]) \tag{2}$$

$$E = e_2^I + (RT/F)\ln([oooo]/[oroo]) \tag{3}$$

$$E = e_3^I + (RT/F)\ln([oooo]/[ooro]) \tag{4}$$

$$E = e_4^I + (RT/F)\ln([oooo]/[ooor]) \tag{5}$$

where [oroo], for example, stands for the concentration of the redox species, in which only heme 2 is reduced. From these equations it is easy to obtain

$$e_1^I - e_2^I = (RT/FI)ln(R_1^I/R_1^I) \tag{6}$$

$$e_2^I - e_3^I = (RT/F)\ln(R_2^I/R_3^I) \tag{7}$$

$$e_3^I - e_4^I = (RT/F)\ln(R_3^I/R_4^I) \tag{8}$$

where R_i^I is the distribution probability of the electron introduced in the first reduction step into heme i. For example, $R_1^I = [rooo]/([rooo] + [oroo] + [ooro] + [ooor])$. Equations (6), (7) and (8) give the relationships between the microscopic redox potentials to determined and R_i^j which are observable. Similar equations were obtained for the fourth reduction step. Such equations also can be deduced for the second and third reduction steps, respectively. Since $\sum_i R_i^j = 1$ and $\sum_j R_i^j = 1$, only 9 out of 16 R_i^j are independent. If we refer to the macroscopic formal potentials, which were determined previously, addional independent equations can be introduced. From eqs. (1), (2), (3), (4) and (5), one has

$$e_i^I = E_1^o + (TR/F)\ln R_i^I \tag{9}$$

and similary

$$e_i^{IV} = E_4^o - (RT/F)\ln R_i^{IV} \tag{10}$$

Consequantly, 11 independent observations and corresponding equations were obtained when E_1^o and E_4^o were taken into account in addition to R_i^j.

If one assume that the effect of the change in the oxidation state of heme i on the redox potential of heme j, which can be called an interacting potential between heme i and

Table 1. Chemical shifts (ppm) of heme methyl singnals in the five macroscopic oxidation states at p²H and 30 °C. Si stands for the *i*-electron reduced state

Signals	Oxidation states				
	S_0	S_1	S_2	S_3	S_4
A	30.54	16.63	12.34	7.22	3.28
B	28.93	20.58	6.10	3.88	3.06
C	20.64	20.37	17.65	6.82	3.18
D	20.34	19.17	15.31	6.20	3.18
E	19.89	17.65	16.14	13.64	3.50
F	19.35	15.29	6.19	4.25	3.20
G	17.91	12.91	5.10	3.63	3.27
H	17.51	10.31	8.09	5.64	3.23
I	16.55	9.66	7.98	5.58	3.24
J	13.34	12.97	12.32		

Table 2. Chemical shifts (ppm) of heme methyl singnals in the five macroscopic oxidition states at p²H 9.0 and 30 °C

Signals	Oxidation states				
	S_0	S_1	S_2	S_3	S_4
A	30.56	10.36	7.81	5.88	3.03
B	29.12	27.26	14.12	5.83	3.00
C	20.53	19.90	17.67	8.66	2.97
D	19.46	18.70	15.37	7.24	3.17
E	20.22	17.34	13.33	12.00	2.95
F	19.08	17.98	10.35	3.91	2.97
G	18.30	17.74	9.66	3.85	3.04
H	17.10	7.07	5.83	5.08	3.10
I	16.27	6.38	5.54	4.23	3.03
J	13.70	14.20	11.38		

j, I_{ij}, is not affected by the oxidation states of the other two hemes, any microscopic potential can be described with the four microscopic potentials and six interacting potentials. Thus, 32 parameters can be reduced to 10. Now, we can determine these parameters analytically because eleven independent equations are more than enough for this purpose.

The interacting potential, I_{ij}, can be defined as follows

$$I_{ij}=e_i^{IIj}-e_i^{I}=e_i^{IIIjK}-e_i^{IIk}=e_i^{IV} \text{ (or } e_i^{IVjkl})-e_i^{IIIkl} \tag{11}$$

where *i, j, k,* and *l* denote heme numberings. It follows, for example, that

$$e_i^{IV}=e_i^{I}+I_{ij}+I_{ik}+I_{il} \tag{12}$$

and

$$I_{ij}=I_{ji} \tag{13}$$

The obtained chemical shifts for p²H 5.2 and p²H 9.0 of the heme methyl group are summarized in Table 1 and Table 2, respectively.

In principle, methyl groups belonging to the same heme should have the same electron-distribution probability. Taking advantage of this property, heme methyl signals can be classified into four groups. The classified electron-distri-

Table 3. Electron-distribution probabillity ($R^i_j=[v(S_{j-1})-v(S_j))/(v(S_0)-v(S_4)]$, $v(S_j)$; chemical shift in oxdation state S_j) calculated from heme methyl chemical shifts at p²H 5.2 and 30 °C. By definition, R^j_i is the distribution probability at heme *i* of the electron introduced in the *j*-th reduction step. Heme methyl groups were assigned to four hemes according to the largest R^j. Heme numbering according to the order of major reduction is given in the rightmost column.

Signals	R^I	R^{II}	R^{III}	R^{IV}	Heme
A	0.510	0.157	0.188	0.145	
H	0.504	0.155	0.172	0.169	h1'
I	0.518	0.126	0.180	0.176	
B	0.323	0.560	0.086	0.032	
F	0.251	0.563	0.120	0.065	h2'
G	0.342	0.533	0.100	0.025	
C	0.015	0.156	0.620	0.208	
D	0.068	0.225	0.531	0.176	h3'
E	0.137	0.092	0.153	0.619	h4'

Table 4. Electron-distribution probaility (see Table 3 for definition) calculated from heme methyl chemical shifts at p²H 9.0 and 30 °C. Heme methyl groups were assigned to four hemes according to the largest R^j. Heme numbering according to the order of major reduction is given in the rightmost colum

Signals	R^I	R^{II}	R^{III}	R^{IV}	Heme
A	0.734	0.093	0.070	0.104	
H	0.716	0.089	0.054	0.141	h1'
I	0.747	0.063	0.099	0.091	
B	0.071	0.503	0.317	0.108	
F	0.068	0.474	0.400	0.058	h2'
G	0.037	0.529	0.381	0.053	
C	0.036	0.127	0.513	0.324	
D	0.047	0.204	0.499	0.250	h3'
E	0.167	0.232	0.077	0.524	h4'

bution probabilities are given in Table 3 and 4.

The scattered values in Table 3 and 4 showed that the contributions of the extrinsic paramagnetic shifts are not negligible. In the estimation of microscopic redox potential, the errors in the electron-distribution probability due to the extrinsic paramagnetic shifts should be minimized. For this purpose, the calculated electron-distribution probability was refined by least-squares fitting under the conditions of $\sum_i R_i^j=1$ and $\sum_j R_i^j=1$. It was carried out using the methyl group, for which all chemical shifts in the five oxidation states could be identified. They are summarized in Table 5.

Thirty two microscopic redox potentials were obtained at p²H 5.2, p²H 7.1 and p²H 9.0 by the combined use of macroscopic redox potentials (from DPP data) with the electron distribution probabilities tabulated in Table 5 (from NMR). The calculation procedure was followed to that reported by Fan *et al.*[6] The results are shown in Table 6 and diagrams

Table 5. The reduction fractions of four hemes at the four redution steps at p^2H 5.2, 7.1 and 9.0, obtained by the least-squares method nuder the condition of $\sum_i R_i^j = \sum_j R_i^j = 1$. R_i^j stands for the reduction fraction of heme i at the j-th reduction step. The chemical shifts of signals A, H, I (heme 4), B, F, G (heme 1), C, D (heme 2) and E (heme 3) were used

Heme No.	Reduction Fraction				Standard
	R^I	R^{II}	R^{III}	R_{IV}	Deviation
p^2H 5.2					
heme 4 (h1')	0.512	0.149	0.178	0.161	0.011
heme 1 (h2')	0.306	0.555	0.100	0.038	0.011
heme 2 (h3')	0.043	0.195	0.573	0.189	0.013
heme 3 (h4')	0.139	0.101	0.148	0.612	0.016
p^2H 7.1					
heme 4 (h1')	0.686	0.050	0.106	0.159	0.009
heme 1 (h2')	0.077	0.533	0.334	0.056	0.009
heme 2 (h3')	0.049	0.225	0.535	0.192	0.010
heme 3 (h4')	0.187	0.193	0.026	0.594	0.012
p^2H 9.0					
heme 4 (h1')	0.732	0.085	0.071	0.113	0.012
heme 1 (h2')	0.059	0.505	0.362	0.074	0.012
heme 2 (h3')	0.042	0.170	0.501	0.288	0.014
heme 4 (h4')	0.167	0.241	0.066	0.526	0.016

Table 6. The microscopic redox potentials at the first and fourth reduction steps (e^I_i and e^{IV}_i, respectively) and interacting potentials (I_{ij}) at p^2H 5.2, p^2H 7.1 and p^2H 9.0. The standard deviations are give in parentheses. Sequential heme numbering is used in the subscripts for the potential notations

	Potential/mV		
	p^2H 5.2	p^2H 7.1	p^2H 9.0
e_1^I	$-267(1)$	$-306(3)$	$-308(5)$
e_2^I	$-318(8)$	$-318(5)$	$-317(9)$
e_3^I	$-288(3)$	$-283(2)$	$-281(3)$
e_4^I	$-253(1)$	$-249(1)$	$-242(1)$
e_1^{IV}	$-264(8)$	$-283(4)$	$-300(4)$
e_2^{IV}	$-305(2)$	$-315(2)$	$-336(1)$
e_3^{IV}	$-336(1)$	$-344(1)$	$-351(1)$
e_4^{IV}	$-301(2)$	$-310(2)$	$-311(3)$
I_{12}	$20(1)$	$41(1)$	$28(1)$
I_{13}	$-10(1)$	$-20(1)$	$-19(1)$
I_{14}	$-7(1)$	$1(1)$	$0(1)$
I_{23}	$-2(1)$	$-9(1)$	$-14(1)$
I_{24}	$-5(1)$	$-29(1)$	$-32(1)$
I_{34}	$-37(2)$	$-33(1)$	$-37(1)$

of Figure 4 through Figure 7.

Here, e_i denoted the microscopic redox potential of heme i. I and IV stand for the first and fourth reduction steps, respectively. Since the second and third reduction steps of each heme have multiple pathways, they were discribed by the combination of the step number (II, III) and the numbering of heme that are kept reduced during the redox process.
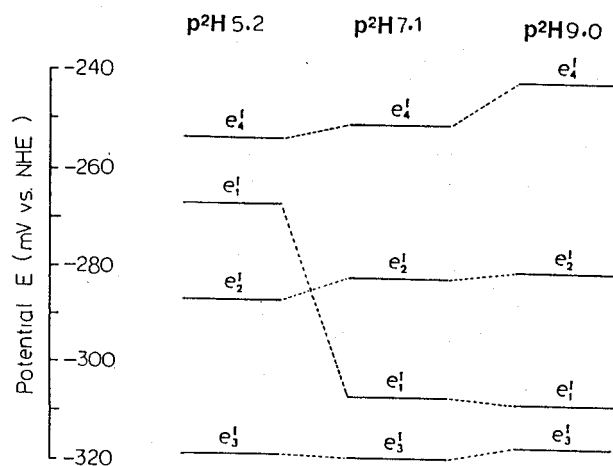

Figure 4. A diagram of the microscopic redox potentials in the first redution process at p^2H 5.2, p^2H 7.1 and p^2H 9.0. NHE and e_i^j denote the normal hydrogen electrode and microscopic formal redox potential of heme i (according to the sequence) at the j-th reduction step, respctively.
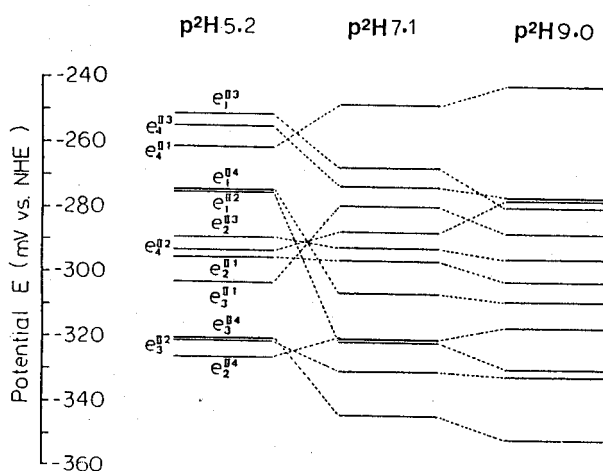

Figure 5. A diagram of the microscopic redox potentials in the second redution process at p^2H 5.2, p^2H 7.1 and p^2H 9.0. e_i^{IIj} denotes microscopic formal redox potential of heme i (according to the sequence), with heme j reduced at the second reduction step.

For example, III_{jk} is the abbreviation of the third reduction step with heme j and k kept reduced.

The microscopic redox potential of heme 1 showed significant p^2H dependence at all reduction steps in acidic range. The interacting potentials (I_{ij}) also are p^2H dependent as shown in Table 6. The remarkable feature of interacting potentials in Table 6 is the large positive value of I_{12} ($=I_{21}$). This means that the presence of an electron at heme 1 (or 2) makes the reduction heme 2 (or 1) much easier. The change of I_{12} was larger in the acidic region than in the alkaline region.

Discussion

The microscopic midpoint redox potentials and interacting potentials of cytochrome c_3 from *D. vulgaris* were shown in
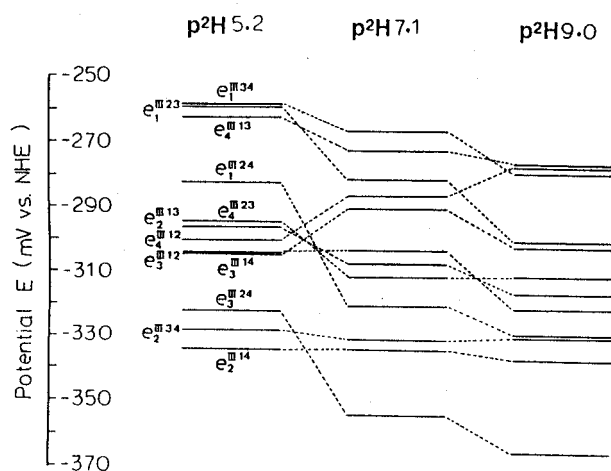
Figure 6. A diagram of the microscopic redox potentials in the third reduction reduction process at p^2H 5.2, p^2H 7.1 and p^2H 9.0. $e_i^{III jk}$ denotes microscopic formal redox potential of heme i (according to the sequence), with heme j and k reduced at the third reduction step.
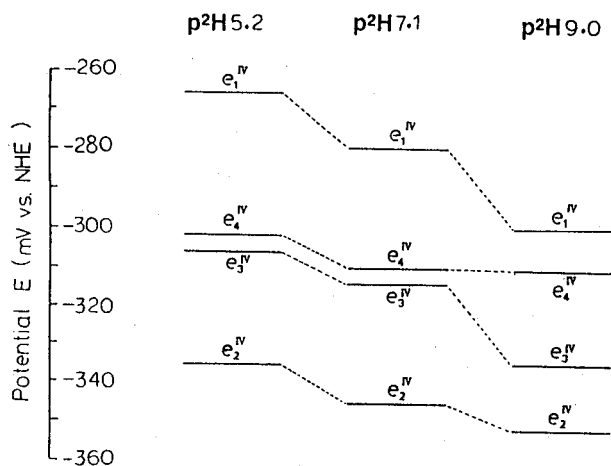

Figure 7. A diagram of the microscopic redox potentials in the fourth reduction process at p^2H 5.2, p^2H 7.1 and p^2H 9.0. See Figure 4 for the abbreviations.

this work to be affected by p^2H.

The p^2H-dependence of the midpoint redox potentials has been reported for many iron-sulfur proteins,[16] and several cytochromes, such as cytochrome c_2,[17] cytochrome c_{551},[18] cytochrome c',[19] and cytochrome c_3.[20,21] The heme propionic acid groups have been postulated as the ionizing groups.[18] The N^1-H group of histidine has also been suggested as a possible candidate.[22]

We now consider the nature of the ionizing groups in cytochrome c_3 from *D. vulgaris* Miyazaki F. Large p^2H dependent shifts of the methyl resonances of heme 1 (h2′) indicate that the ionizable group is close to the heme. Actually, the titration curves of 6-propionate β-CH_2 of heme 1 (h2′) were found to be similar to those of the methyl groups of heme 1 (h2′) in the intermediate oxidation states. Thus, protonation of this propionic acid might influence the redox potentials of heme 1 (h2′) in acidic range. The 6-propionate group of heme

1 (h2′) is less exposed and less hydrogen-bonded than other propionate groups of *Dv*MF cytochrome c_3. Inspection of the crystal structure shows that the imidazole ring of His 67 form hydrogen bonds with the carboxyl groups of Asp 71 and the propionate of heme 2. The chain of hydrogen bonds mentioned above could contribute significantly to the conformation of the entire protein.[23] Most heme methyl signals in intermediate oxidation states shifted at around p^2H 8.5 (in Figure 1), close to the pK_a value of His 67 (C2-H, C4-H). Thus protonation of His 67 might influence the redox potentials of cytochrome c_3 from *D. vulgaris* Miyazaki F in basic range.

The fact that the heme midpoint redox potentials and interacting potentials are sensitive to p^2H of the solution, supports the idea that cytochrome c_3 plays a complex role in a cell. The reaction *in vivo* would be carried out at different redox potentials and also possibly involving proton transfer. Although a mechanism for the interheme interaction in cytochrome c_3 is not yet elucidated, it is resonable to speculate that a conformational change of the protein induced by the redox reaction at a particular heme would influence the midpoint redox potentials of other hemes and also the pK_a of dissociable groups.

The p^2H effect on the midpoint redox potentials of the heme might also play an important role. Indeed, protons produced by the hydrogenase could temporarily increase the midpoint redox potentials of the heme, favoring the subsequent acceptance of electrons. Alternatively, the release of protons by cytochrome c_3 could facilitate its subsequent oxidation. By this mechanism, the proton transfer would assist the electron transfer between cytochrome c_3 and hydrogenase, which itself contains redox centers with p^2H-dependent midpoint redox potentials.

References

1. Niki, K.; Kawasaki, Y.; Higuchi, Y.; Yasuoka, N. *Langmuir* **1987**, *3*, 333.
2. Hinnen, C.; Parsons, R.; Nagai, Y. *Bull. Chem. Soc. Japan,* **1954**, *27*, 564.
3. Sagara, T.; Nakajima, S.; Akutsu, H.; Niki, K. *J. Electroanal. Chem.* **1991**, *297*, 271.
4. Nakahara, Y.; Kimura, K.; Inokuchi, H.; Yagi, T. *Chem. Lett* **1979**, 877.
5. Kimura, K.; Sato, N.; Hino, S.; Yagi, T. Inokuchi, H. *J. Am. Chem. Soc.* **1978**, *100*, 6564.
6. Fan, K.; Akutsu, H.; Kyogoku, Y.; Niki, K. *Biochemistry* **1990**, *29*, 2257.
7. Fan, K.; Akutsu, H.; Niki, K.; Higuchi, N.; Kyogoku, Y. *J. Electroanal. Chem.* **1990**, *278*, 295.
8. Park, J.-S.; Kano, K.; Niki, K.; Akutsu, H. *FEBS Lett.* **1991**, *285*, 149.
9. Higuchi, Y.; Kusunoki, M.; Matsuura, Y.; Yasuoka, N.; Kakudo, M. *J. Mol. Biol.* **1984**, *172*, 109.
10. Postgate, J. R. *The Sulphate-reducing Bacteria*, 2nd ed.,

826 *Bull. Korean Chem. Soc.* **1996**, Vol. 17, No. 9

Joon Y. Lee and Laurence A. Belfiore

Cambridge University Press: Cambridge, U. K., 1984, 76.

11. Park, J.-S.; Kang, S. W. *Bull. Korean Chem. Soc.* **1993**, *14*, 588.

12. Yagi, T.; Maruyama, K. *Biochem. Biophys. Acta*, **1971**, *243*, 214.

13. Park, J.-S. *Bull. Korean Chem. Soc.* **1995**, *16*, 1139.

14. Niki, K.; Kobayashi, Y.; Matsuda, H. *J. Elecroanal. Chem.* **1984**, *178*, 333.

15. Kimura, K.; Nakajima, S.; Niki, K.; Inokuchi, H. *Bull. Chem. Soc. Jpn.* **1985**, *58*, 1010.

16. Maggliozzo, R. S.; McIntosh, B. A.; Sweeney, W. V. *J. Biol. Chem.* **1982**, *257*, 3506.

17. Pettigrew, G. W.; Meyer, T, E.; Bartsch, R. G.; Kamen, M. D. *Biochim. Biophys. Acta*, **1975**, *430*, 197.

18. Moore, G. R.; Pettigrew, G. W.; Pitt, R. C.; Williams, R. J. P. *Biochim. Biophys. Acta*, **1980**, *590*, 261.

19. Barakat, R.; Strekas, T. *Biochim. Biophys. Actsa*, **1971**, *679*, 393.

20. Moure, J. J. G.; Santos, H.; Moura, I.; LeGall, J.; Moore, G. R.; William, R. J. P.; Xavier, A. V. *Eur. J. Biochem.* **1982**, *127*, 151.

21. Santos, H.; Moura, J. J. G.; LeGall, J.; Xavier, A. V. *Eur. J. Biochem.* **1984**, *141*, 283.

22. Gadsby, P. M. A.; Thomson, A. J. *FEBS Lett.* **1982**, *150*, 59.

23. Park, J.-S.; Enoki, M.; Ohbu, A.; Fan, K.; Kyogoku, Y.; Niki, K.; Akutsu, H. *J. Mol. Struct.* **1991**, *242*, 343.

Chemical Reactions in Solid State Complexes of 1,2-Polybutadiene and Palladium Chloride: High Temperature Infrared Study

Joon Y. Lee[†] and Laurence A. Belfiore

Department of Textile Engineering, Kyung Hee University, Kyungki-do 449-701, Korea

Polymer Physics and Engineering Laboratory, Department of Chemical and Bioresource Engineering,
Colorado State University, Fort Collins, Colorado, USA 80523

Received May 7, 1996

Fourier transform infrared (FTIR) temperature studies were performed to examine the microstructural changes that occur in annealing process of the thin films of 1,2-polybutadiene (1,2-PBu)/palladium chloride (PdCl$_2$) complex. The disappearance of the infrared absorption intensities at 1640, 1418, 994 and 910 cm^{-1} signifies the consumption of 1,2-vinyl groups of 1,2-PBu. The progressive loss of unsaturation and production of methyl groups as a function of temperature were identified by the enhanced infrared absorption intensities at 1447 and 1375 cm^{-1}. The loss of pendent carbon-carbon double bond is considered to involve both palladium-catalyzed addition reaction and thermally induced cyclization.

Introduction

In a recent paper,[1] a reactive blending through transition metal-olefin coordination complex formation in diene polymers was presented. Upon mixing these diene polymers with a *trans*-square-planar transition metal salt, *i.e.*, bis(acetonitrile) dichloropalladium(II), PdCl$_2$(CH$_3$CN)$_2$, effective coordination cross-links formed because the acetonitrile ligands of the palladium salt are displaced by olefinic pendent groups of the polymers. The addition of palladium chloride to linear diene polymers containing olefinic side groups followed by high temperature annealing generated networks with greatly enhanced thermal and mechanical properties. The macroscopic results could be explained by palladium-catalyzed addition reactions that chemically crosslink linear chains through olefinic side groups. It was proposed that a Heck like reaction mechanism is operative to produce linear chemical cross-links between main chains. The reaction mechanism has been discussed in somewhat plausible manner based on the previous studies of the chemistry of palladium compounds in which the palladium catalyzed chemical cross-links occur in solid state complexes of 1,2-polybutadiene (1,2-PBu) and palladium chloride (PdCl$_2$) under annealing process.

FTIR spectroscopy has been useful as a diagnostic probe of the various types of chemical reactions that could occur in these solid films. In this report, we will present the above mentioned chemical reactions in more detail in the temperature range from room temperature to 200 ℃ by *in-situ* high temperature infrared spectroscopy.

Experimental Section

Atactic 1,2-PBu was supplied by Goodyear Tire & Rubber Co. (Akron, OH), by the courtesy of Dr. Adel F. Halasa. The sample was used as received without any additional purification. The microstructure of 1,2-PBu investigated in this study

---

†To whom correspondence should be addressed.